Spatial modelling of the variability of the soil moisture regime at the landscape scale in the southern Qilian Mountains, China

C-Y. ZHAO [1], P-C. QI [2], Z-D. FENG [2]

1 Key laboratory of arid and grassland agroecology (Ministry of Education), Lanzhou University, Lanzhou 730000, China.

E-mail: nanzhr@lzb.ac.cn

2 Key laboratory of western China’s environment systems (Ministry of Education), Lanzhou University, Lanzhou 730000, China.

Abstract

The spatial and temporal variability of the soil moisture status gives an important base for the assessment of ecological (for restoration) and economic (for agriculture) conditions at micro- and meso-scales. It is also an essential input into many hydrological processes models. However, there has been a lack of effective methods for its estimation in the study area. The aim of this study was to determine the relationship between the soil moisture status and precipitation and topographic factors. First, this study compared a linear regression model with interpolating models for estimating monthly mean precipitation and selected the linear regression model to simulate the temporal-spatial variability of precipitation in the southern Qilian Mountainous areas of the Heihe River Basin. Combining topographic index with the distribution of precipitation, we calculated the soil moisture regime in the Pailugou catchment, one representative comprehensive research catchment. The modeled results were tested by the observed soil water content for different times. The correlation coefficient between the modeled soil moisture status and the observed soil water content is quite high, assuring our confidence in the spatially-modeled results of the soil moisture status. The method was applied to the southern Qilian Mountainous regions. Therefore the modelled distribution of the soil moisture status reflected the interplay of the local topography and landscape climate processes. The driest sites occur on some ridges in northern part and western part of the study area, where have small accumulating flow areas and low precipitation rates. The wettest sites are registered in the low river valley of the Heihe River and its major tributaries in the eastern part due to large accumulating flow areas and higher precipitation rates. Temporally, the bigger variation of the soil moisture status in the study occurs in July and smaller difference appears in May.

Keywords: soil moisture status; precipitation; linear regression; topographic index; Qilian Mountains; Landscape scale

1 Introduction

The Heihe River Basin, the second largest inland river basin in the arid regions of northwestern China, consists of three major geomorphic units: the southern Qilian Mountains, the middle Hexi Corridor, and the northern Alxa Highland. The southern Qilian Mountains are hydrologically and ecologically the most important unit because of the functions as the water source to support the irrigating agriculture in the Hexi Corridor and also to maintain the ecological viability in the northern Alxa Highland. With the rapid growth of population, agricultural irrigation areas increasingly spread in the middle Hexi Corridor. As a result, the already-existing conflict between economic use of the water here and ecological demand of the water in the Alxa Highland has been recently exacerbated. How to resolve the conflict and coordinate the development in economy and ecological environments becomes the focus of attention in the Heihe River basin. Many researchers have dealt with water resources, such as water resources carry capacity (Ji, et al., 2006), ecological requirement water (Zhao, et al., 2005; Zhao et al., 2010), the runoff amount of the Heihe River and its variation (Wang, et al., 2009), methods of irrigation and so on. The water resources are very scarce in the Heihe River basin, and the runoff from the southern Qilian Mountains approximately represents the water resources amount of the middle Hexi Corridor and the northern Alxa Highland. Therefore, accurate estimation of runoff from Qilian Mountainous watersheds is an urgent need for answering Heihe River water resources carry capacity and for water management and planning. To accomplish the needed runoff estimation in the upper reaches, the soil moisture status has to be spatially and temporally portrayed, as it is a critical state variable in hydrological models (Liang et., 1994; Wignosta et al., 1994; Famiglietti and Wood, 1994; Li & Islam, 1999). The temporal and spatial variations in soil moisture depend on availability of high-resolution ground-based monitoring (Li & Islam, 2002). Unfortunately, ground-based methods (e.g. neutron thermalization, oven-dry method) are much too labor-intensive to maintain for a large area (e.g., the entire southern Qilian Mountains). Thus, in this study the relationship between the temporal and spatial variation of soil moisture is determined by establishing its controlling factors, e.g. precipitation. Precipitation fields on a regular grid and in digital forms are required for spatial mapping of soil moisture. Accurate rainfall data only exist for irregularly distributed rain gauges and the meteorological stations, as a result of which values at any other point in the terrain must be inferred from neighbouring stations or from relationships with other variables (Marquínez et al., 2003). There are many methods of interpolating precipitation from monitoring stations to grid points (Dirks et al., 1998; Goovaerts, 2000; Wei, et al., 2005; Price et al., 2000; Guenni & Hutchinson, 1998). Basic techniques ues only the geographic coordinates of the sampling points and the value of the measured variable. However, the study area is one in which these methods have not been applied previously. In addition, regression models are using only additional information as regression models between precipitation and various topographic variables such as altitude, latitude, continentality, slope, orientation or exposure (Basist et al., 1994; Goodale et al., 1998; Ninyerola et al., 2000; Wotling et al., 2000; Weisse & Bois, 2001). But few researchers could interpolate precipitation by regression models in the study area because of unavailable digital elevation models (DEM). Fortunately, significant progress in this area has recently been achieved through the development of a high-resolution DEM with a resolution of 10m×10m by the remote sensing laboratory of Cold and Arid Regions Environmental and Engineering Research Institute, CAS. The other controlling factors of soil moisture and topographic factors, are best delineated by the DEM at the resolution that closely matches the smallest orographic scale supported by the data.

This study sought to develop the relationships between soil moisture and its controlling factors (i.e., precipitation and topographic variables) in order to map the soil moisture status across the southern Qilian Mountains. In the following sections we will present the various steps that lead to the mapping of the soil moisture regime: (1) use of available data; (2) determination of the best model for modelling the areal distribution of precipitation; (3) definition of the wetness index and GIS realization of the wetness index model; (4) mapping of the soil moisture status distribution; and finally (5) validation of the results.

2 Materials and methods

2.1 Study area

The study area, one portion of the Qilian Mountains within the Heihe River Basin, is located between $98^{\circ}34'$ - $101^{\circ}11'$ E and $37^{\circ}41'$ - $39^{\circ}05'$ N and covers an area of approximately 10, 009 km^2, with the elevation ranging from 2000 to 5500m a.s.l. Administratively, the major part of the study area is in Gansu Province and a small part in Qinghai Province (Fig. 1). The mean annual precipitation increases with the increasing elevation (from 250 to 700mm). The inter-annual variability in the precipitation is as high as 80%, and over 88% of the precipitation falls between May and September. Figure 2 shows the pattern of rainfall over the year in Zhamashike meteorological station (one representative meteorological station in the study area). The mean annual temperature decreases with the increasing elevation (from 6.2 to -9.6°C). The vegetation distribution closely follows the temperature- and precipitation-determined heat-water combinations in the mountains. They are (from low to high elevations): desert steppe, forest steppe, sub-alpine shrubby meadow, alpine cold desert, and ice/snow zone. In addition to the obvious vertical zonality, horizontal zonality also exits due to precipitation and air temperature differences from the south to the north and from the east to the west. Generally, precipitation decreases from the east to the west and increases from the north to the south but the temperature is reverse in the study area.

Figure 1 The location of the study area, meteorological stations and rain gauges.

Figure 2 Distribution of monthly mean precipitation in Zhamashike meteorological station (1957-1995).

2.2 Data collection

The monthly mean precipitation data (from 1957 to 1995) were obtained from 43 stations, including meteorological stations and rain gauges located within the study area and the surrounding areas. The locations and the altitudes of these stations were measured with a global positioning system (GPS) and an elevation meter. Among them, 30 stations were chosen to develop the regression model or to use for interpolating and other 13 stations were remained to test the models (Fig. 1). Soil was sampled at four depths (0-10, 10-20, 20-40, 40-60 cm) from May to September in 2003 and 2004 in Pailugou catchment (one representative comprehensive research catchment in the study area located at 38.55° N, 100.30° E). Soil moisture was measured by the conventional oven-dry method. DEMs of the study area and Pailugou catchment were obtained from the remote sensing laboratory of Cold and Arid

Regions Environmental and Engineering Research Institute, CAS.

2.3 Description of models

Hydrological prediction at the micro- and meso-scales is intimately dependent on the ability to characterize the spatial variability of the soil water content. However, soil moisture exhibits drastic temporal and spatial variations even in a small catchment. In mountainous terrains, the soil water distribution is controlled by vertical and horizontal water divergence and convergence, infiltration recharge, and evapotranspiration. The latter two terms are affected by solar insolation and the vegetation canopy that vary strongly with exposure in arid areas. The divergence/convergence term is dependent on hill-slope position (Moore et al., 1993). Considering the hill-slope position, most index approaches for predicting the spatial distribution of soil water can be expressed as (Beven and Kirkby, 1979):

$$IN_1 = ln\ (a/tan\beta) \qquad (1)$$

where IN_1 is the wetness index, α the contributing area and β the local slope of the terrain. The soil water content is not only affected by the divergence/convergence of water but also affected by evapotranspiration. In arid areas, evapotranspiration is obviously different in different aspects because of variations of insolation. A modified wetness index is defined by merely introducing the factor of aspect (A), an appropriate surrogate of potential insolation (Grayson et al., 1997; Gomez-Plaza et al., 2001). Then, the Eq.(1) becomes:

$$IN_2 = ln\ (a/tan\ \beta) \times cosA \qquad (2)$$

where IN_2 is the modified wetness index and A the aspect.

The soil moisture index at landscape scales is determined by high-resolution spatial distributions of precipitation and DEM-based topographic factors (Dymond and Johnson, 2002) and given as the following:

$$IN_3 = ln(a/tanB) \times cosA \times P_i \tag{3}$$

where IN_3 is the soil moisture index in every month, P_i the monthly mean precipitation. Equation(3) requires four parameters: slope, aspect, the specific catchment area (catchment area draining across a unit width of contour) and precipitation. Topographical parameters such as slope (β), aspect (A), and the contributing area (α) are computed from DEM. Precipitation is an important parameter and must be accurately estimated.

We here used five methods to simulate the temporal and spatial distribution of precipitation in the southern Qilian Mountains, i.e. linear regression, inverse distance weighted (IDW), ordinary kriging (OK), trend and spline. The regression model derived by regression analyses can predict annual, monthly precipitation as functions of elevation and geographical coordinates (Wei et al., 2005; Michaud et al., 1995). By the analysis of the precipitation data with their elevation and geographical coordinates in the study, a linear regression relationship between the monthly mean rainfall and locational/topographic factors is presented as:

$$P_i = a + bH + cY + dX \quad (4)$$

where H is the altitude in meter, Y the latitude in degree, X the longitude in degree and a, b, c, d the regression coefficients (Table 1).

Table 1

Besides the regression model, four conventional interpolation methods, inverse distance weighted (IDW), spline, ordinary kriging (OK), and trend, were tested. IDW estimates the value of an unsampled area as a weighted average of a defined number of neighborhood points, or area, and the weight assigned to each neighborhood point diminishes as the distance to the neighborhood point increases (Lloyd, 2005). Spline interpolators have been widely used in developing climatic surfaces from sparse observation points (Tsanis and Gad, 2001). The interpolated surface based on spline (a) passes exactly through the data points and (b) has a minimum curvature. OK is a geostatistical procedure that uses a variogram model, which describes the spatial continuity of the input data to estimate values at unsampled locations (Isaaks and Srivastava, 1989). The variability between samples as a function of distance (i.e., semivariance) is evaluated and modeled prior to kriging (Wackernagel, 1995). The trend surface interpolator uses a polynomial regression to fit a least-squares surface to the input points. It creates smooth surfaces. The surface generated will seldom pass through the original data points since it performs the best fit for the entire surface.

3 Results and discussion

3.1 Wetness indexes

Topographical parameters, such as slope, aspect (A) and the contributing area were computed from DEM. The aspect is expressed in positive degrees from 0 to 360, measured clockwise from the north. The maps of the wetness index (IN_1) and the modified wetness index (IN_2) in the southern Qilian Mountains were obtained from the models using ARC/INFO + grid (Fig. 3). The simulated wetness indexes were validated by observed data. We found that IN_1 was able to explain between 34% and 38% of the spatial variability of soil moisture, but if the aspect was considered as a complementary factor, this capacity increased up to 69.5%. The results were supported by some researches (Moor et al., 1988; Gómez-Plaza et al., 2001). However, Eq. (1) and Eq. (2) only take the topographic factors into account and suppose a homogenous precipitation in the small catchment. In fact, precipitation shows dramatically differences at landscape scales in the study area. It increases from the north to the south, from the lower altitude to the higher altitude, and decreases from the east to the west. In turn, the soil moisture status exhibits a spatially inhomogeneous arrangement in the landscape due to precipitation. Therefore, precipitation must be considered.

Figure 3 The distribution of wetness indexes (IN_1 and IN_2) in the southern Qilian Mountains.

3.2 Spatial and temporal distributions of precipitation

Prediction on the locations of the validation points and the measured values at these locations were compared by three criteria: the mean error (ME), the mean absolute error (MAE) and the root mean square error (RMSE). ME indicates the degree of bias, MAE provides a measure of how far the estimate can be in error, ignoring the sign, and RMSE provides a measure that is sensitive to outliers. A summary of the errors obtained from the criteria was presented in Table 2. ME was relatively low for IDW, OK, trend and linear regression, but was generally lowest for the linear regression model. The linear regression and OK methods gave the lower MAE and RMSE. The spline gave consistently poor performances. For five methods, there were substantial variations in RMSE through the year (Fig. 4). The highest errors occurred from July to September and the lowest values from October to February, which probably reflected the greater precipitation differences across the region in summer. From Jun. to August, the linear regression performed better than OK. Thus the conclusions are as follows: on average over the year, larger predictions errors were obtained by the spline, the trend and IDW methods that ignore elevation factors, with the worst results produced by the spline. It was noteworthy that for several months (from January to May, from September to December), OK yielded smaller prediction errors than the linear regression of precipitation against elevation and locational/topographic factors.

Table 2

Figure 4 Validation RMSE for monthly mean precipitation averaged across 13 test stations for five methods.

As mentioned above, over 88% of the precipitation falls between May and

September and over 63% between June and August in the southern Qilian Mountainous areas of the Heihe River Basin. We were here focusing on the spatial distribution of precipitation during the ecologically meaningful time period, i.e., growing seasons approximately from May to August. Our comparison between these models' performances demonstrated that the linear regression model did the best job during the ecologically meaningful time period. The best performance of the linear regression in the study area made this model the best choice. A series of spatial-distribution maps of precipitation were obtained by the regression model (Fig. 5). Figure 5 showed that lower precipitation values were registered in the low valleys of the Heihe River and the northwest part, and higher precipitation values appeared in the southeast part where the altitude and longitude depended precipitation is higher. Figure 5 also showed that precipitation value had temporal variations during growing seasons (i.e. from May to August), highest precipitation value, ranging from 46mm to 145.4mm, appearing in the July, and the lowest precipitation value, from 25.2mm to 64.5 mm, being seen in May.

Figure 5 Distribution of monthly mean precipitation in southern Qilian Mountains from May to August.

3.3 Temporal and spatial distribution of soil moisture status in the southern Qilian Mountains.

The soil moisture data are fairly sparse in the study area. We could not collect the soil moisture data except in Pailugou catchment, one representative comprehensive research catchment. The catchment is about 10 km^2 in area situated at 38.55^{o} N and

100.30^o E and has a weather station with a pluviometer, wind speed and direction, wet and dry bulb temperature. The soil moisture status was simulated using Eq. (3) by supposing the homogenous precipitation in the catchment. To test the spatially-modeled results of the soil moisture status in Pailugou catchment, we compared the observed results for 4 months at 15 sample plots with the spatially-modeled results for the corresponding months and sample plots. The correlation coefficients (R^2) are from 0.60, 0.76, 0.67, 0.69 for May, June, July and August respectively (Fig. 6). These assure our confidence in the spatial model (i.e. equation 3) of the soil moisture status. In addition to topography, the land use type is another important factor controlling soil water patterns, which means that difference in vegetations resulting from different land use types was one of the major factors influencing soil moisture variability. However, the factor of vegetations is not included in Eq. (3). How to improve the model to estimate the soil moisture status is an objective of our future study.

Figure 6 Scatter plots of observed soil moisture content and modeled soil moisture status from May to August

The same strategies were employed to estimate the soil moisture status of the southern Qilan Mountains areas (Fig. 7). The distributions of the soil moisture status in the study area reflected the interplay of the local and landscape climate processes. As viewed from a small scale, the gentle bases of long hill-slopes had more moisture than the steep short sites due to its larger catchment areas, and the south-facing slope had less moisture than the north-facing slope because it got more insolation on the dryness of the matrix soil water. From the landscape scale viewpoint, the moisture increased from the north to the south and from the west to the east due to the precipitation increase. Figure 7 showed that the driest sites (IN_3 from –1.54 to –0.64) occurred on some ridges in the northern part and the western part of the study area, which had very small catchment areas and small precipitation. The wettest sites (IN_3 from 2.00 to 0.75) were registered in the low valleys of the Heihe River and its major tributaries in the eastern part due to large accumulating flow areas and more precipitation. The bigger variation of the soil moisture status in the study occurred in July and smaller difference appeared in May.

Figure 7 Distribution of monthly mean soil moisture status in southern Qilian Mountains from May to August.

4 Conclusions

Accurate prediction of the soil moisture status at the large scale is of crucial interest to hydrology and agronomy related studies in the southern Qilian Mountains. However, soil moisture data are not available and ground-based methods (e.g. neutron thermalization, oven-dry method) are far too labor-intensive to maintain for the large area (e.g., the entire southern Qilian Mountains). Therefore, it is very important to develop more descriptive models of the soil moisture status. We can draw some conclusions from the approach:

1. Equation (3) was used to predict the variability of the soil moisture status in the study area and the model was validated by Pailugou catchment. The results of validation assured our confidence in the spatially-modeled results of the soil moisture

status. But one important factor affecting soil moisture is vegetation types which was excluded in the model.

2. Equation (3) includes two terms, the wetness index and precipitation. The model of the wetness index in Eq. (2) is universal. So accurate estimations of precipitation are very important to estimate the soil moisture state. We thus selected five methods to simulate the temporal-spatial distributions of precipitation in the study. By comparison, the best performance of the linear regression in the study area made this model the best choice.

3. A series of soil moisture status maps were obtained by Eq. (3). Generally, the gentle bases of long hill-slopes had more moisture than the steep short sites because they had larger catchment areas. The south-facing slope had less moisture than the north-facing slope because it got more insolation on the dryness of the matrix soil water. The driest sites occurred on some ridges in the northern part and the western part of the study area, where have small accumulating flow areas and small precipitation. The wettest sites were registered in the low valleys of the Heihe River and its major tributaries in the eastern part due to large accumulating flow areas and more precipitation.

4. Care must be exercised in appling the equation (3) to predict the distribution of soil moisture status at large scale in Chinese Loess Plateau due to three natural factors: steeply-sloped topography with gullies, fine-textured loessial soils and most importantly, unique hydrogeomorphic conditions. The unique hydrogeomorphic conditions refer to the rainfall intensity often exceeds the soil infiltration capacity.

Gullies are ubiquitous landscape features on natural slopes, which affect water divergence and convergence. It is impossible to obtain high accuracy of DEM to depict slope (β), aspect (A), and the contributing area (α). The unique hydrogeomorphic conditions can not make initial surface saturation occurs.

Acknowledgements

This project was supported by Nation Natural Science Foundation of China (No. 40671067, No. 30770387); National Environmental Protection Commonweal Project of China(NEPCP 200809098).

References

1. Basist, A., Bell, G. D., and Meentemeyer, V.: Statistical relationships between topography and precipitation patterns, J.Climate, 7, 1305-1315, 1994.
2. Beven, K. J., and Kirkby, M. J.: A physically based, variable contributing area model of basin hydrology, Hydrological Science Bulletin, 24, 43-69, 1979.
3. Dirks, K. N., Hay, J. E., Stow, C. D., and Harris, D.: High-resolution studies of rainfall on Norfolk Island part II: interpolation of rainfall data, J. Hydrol., 208, 187-193, 1998.
4. Dymond, C. C., and Johnson, E. A.: Mapping vegetation spatial patterns from modeled water, temperature and solar radiation gradients, Journal of Photogrammetry and Remote Sensing, 57, 69-85, 2002.
5. Famiglietti, J. S., and Wood, E. F.: Multiscale modeling of spatially variable water and energy balance processes, Water Resour. Res., 30, 3061-3078, 1994.
6. Gómez-Plaza, A., Martínez-Mena, M., Albvaladejo, J., and Castillo, V. M.: Factors regulating spatial distribution of soil water content in small semiarid catchments, J. Hydrol., 253, 211-226, 2001.
7. Goodale, C. L., Alber, J. D., and Ollinger, S. V.: Mapping monthly precipitation, temperature and solar radiation for Ireland with polynomial regression and digital elevation model, Clim. Res., 10, 35-49, 1998.

8. Goovaerts, P.: Geostatistical approach for incorporating elevation into the spatial interpolation of rainfall, J. Hydrol., 228, 113-129, 2000.

9. Grayson, R. B., Western, A. W., and Chiew, F. H. S.: Preferred states in spatial soil moisture pattern: local and nonlocal controls, Water Resour. Res. 33, 2879-2908, 1997.

10. Guenni, L., and Hutchinson, M. F.: Spatial interpolation of the parameters of a rainfall model from ground-based data, J. Hydrol., 212-213, 335-347, 1998.

11. Isaaks, E. H., and Srivastava, R. M.: An introduction to applied geostatistics, Oxford University Press, New York, 516pp., 1989.

12. Ji, X. B, Kang, E., and Chen R. S.: Analysis of Water Resources Supply and Demand and Security of Water Resources Development in Irrigation Regions of the Middle Reaches of the Heihe River Basin, Northwest China, Agricultural Sciences in China, 5, 130-140**,** 2006.

13. Li J. K., and Islam S.: On the estimation of soil moisture profile and surface fluxes partitioning from sequential assimilation of surface layer soil moisture, J. Hydrol., 220, 86-103, 1999.

14. Li J. K., and Islam S.: Estimation of root zone soil moisture and surface fluxes partitioning using near surface soil moisture measurements, J. Hydrol., 259, 1-14, 2002.

15. Liang, X., Lettenmaier, D. P., Wood, E. F., and Burges, S. J.: A simple hydrologically based model of land surface water and energy fluxes for general circulation models, J. Geoph. Res., 99, 14, 415-428, 1994.

16. Lloyd, C. D.: Assessing the effect of integrating elevation data into the estimation of monthly precipitation in Great Britain, J. Hydrol., 308, 128-150, 2005.

17. Marquínez J., Lastra J., and García P. : Estimation models for precipitation in mountainous regions: the use of GIS and multivariate analysis, J. Hydrol., 270, 1-11, 2003.

18. Michaud, J. D., Auvine, B. A., and Penalba, O. C.: Spatial and elevation variations of summer rainfall in the southwestern United States, J. Appl. Meteorol., 34, 2689-2703, 1995.

19. Moore I. D., Turner A. K., Wilson J. P., Jenson S. K., and Band L. E.: GIS and land-sruface-subsurface process modeling. In: Goodchild M. F., Parks B. V. Steyaert L. T. (eds) Environmental modeling with GIS. New York. pp 196-229, 1993.
20. Moore, I. D., Burch, G. J., and Mackenzie, D. H.: Topographic on the distribution of surface soil water and the location of ephemeral gullies, Trans. Am. Soc. Agric. Eng., 31, 1098-1107, 1988.
21. Ninyerola, M., Pons, X., and Roure, J. M.: A methodological approach of climatological modelling of air temperature and precipitation through GIS techniques, Int. J. Climatol., 20, 1823-1841, 2000.
22. Price D. T., McKenney D. W., and Nalder I. A.: A comparison of two statistical methods for spatial interpolation of canadian monthly mean climate data, Agr. Forest Meteorol., 101, 81-94, 2000.
23. Tsanis, I. K., and Gad, M. A.: A GIS Precipitation method for analysis of storm kinematics, Environ. Modell. Softw., 16, 273-281, 2001.
24. Wackernagel, H.: Multivariate Geostatistics, Springer-Verlag, Berlin, 256pp, 1995.
25. Wang, J.S., Feng, J. Y., and Yang, L. F.: Runoff-denoted drought index and its relationship to the yields of spring wheat in the arid area of Hexi corridor, Northwest China, Agricultural water management, 96, 666-676, 2009.
26. Wei H., Li J., and Liang T.: Study on the estimation of precipitation resources for rainwater harvesting agriculture in semiarid land of China, Agr. Water Manage., 71, 33-45, 2005.
27. Weisse, A. K., and Bois, P.: Topographic effects on statistical characteristics of heavy rainfall and mapping in the French Alps, J. Appl. Meteorol., 40, 720-740, 2001.
28. Wignosta, M. S., Vail, L. W., and Lettenmaier, D. P.: A distributed hydrology-vegetation model for complex terrain, Water Resour. Res., 30, 1665-1679, 1994.
29. Wotling, G., Bouvier, C., Danloux, J., and Fritsch, J. -M.: Regionalization of

extreme precipitation distribution using the principal components of the topographical environment, J. Hydrol., 233, 86-101, 2000.

30. Zhao Chuanyan, Nan Zhongren, and Cheng Guodong: Methods for estimating irrigation needs of spring wheat in the middle Heihe basin, China, Agr. Water Manage., 75, 54-70, 2005.

31. Zhao, W.Z., Liu, B., and Zhang, Z. H.: Water requirements of maize in the middle Heihe River basin, China, Agricultural water management, 97, 215-223, 2010.

Table 1. Monthly linear regression coefficients and R^2 needed to calculate monthly mean precipitation using altitude (H), latitude (Y) and longitude (X) for the southern Qilian Mountains ($P = a + bH + cY + dX$).

time	a	b	c	d	R^2
Jan.	**-19.811**	**0.000260**	**-0.051**	**0.231**	**0.207**
Feb.	**-70.701**	**0.001103**	**0.221**	**0.626**	**0.331**
Mar.	**-249.545**	**0.003390**	**0.433**	**2.336**	**0.406**
Apr.	**-16.862**	**0.004009**	**-4.289**	**1.879**	**0.584**
May	**408.331**	**0.009569**	**-12.540**	**0.869**	**0.810**
Jun.	**530.716**	**0.021000**	**-13.656**	**0.016**	**0.863**
Jul.	**689.699**	**0.029650**	**-12.485**	**1.018**	**0.870**
Aug.	**495.902**	**0.018520**	**-19.839**	**2.869**	**0.879**
Sep.	**196.940**	**0.009100**	**-15.049**	**4.003**	**0.856**
Oct.	**-5.170**	**0.002153**	**-5.737**	**2.341**	**0.841**
Nov.	**-136.015**	**0.000984**	**0.240**	**1.283**	**0.455**
Dec.	**-81.180**	**0.000480**	**0.493**	**0.627**	**0.166**
Annual	**1742.001**	**0.097260**	**-87.915**	**17.197**	**0.861**

Table 2. Validation errors averaged across 13 test sites for the five interpolation methods in each month.

	Models	Jan	Feb	Mar	Apr	May	Jun	Jul	Aug	Sep	Oct	Nov	Dec
ME	IDW	**0.20**	**0.95**	**2.56**	**0.83**	**-1.2**	**5.97**	**-2.58**	**1.28**	**-4.56**	**0.3**	**-0.68**	**0.59**
	TREND	**0.31**	**0.72**	**1.32**	**5.33**	**0.40**	**0.64**	**0.31**	**0.72**	**1.32**	**5.33**	**0.40**	**0.64**
	OK	**0.22**	**0.97**	**2.54**	**1.48**	**0.35**	**6.73**	**-2.23**	**2.66**	**-3.78**	**0.75**	**-0.65**	**0.58**
	SPLINE	**0.42**	**1.16**	**3.65**	**2.59**	**1.27**	**9.98**	**-0.94**	**4.5**	**-3.3**	**1.02**	**-0.38**	**0.7**
	REGRESSION	**0.32**	**1.04**	**2.3**	**0.36**	**-1.51**	**6.15**	**-3.56**	**-0.23**	**-6.09**	**-0.57**	**-0.75**	**0.7**
MAE	IDW	**0.84**	**1.56**	**4.46**	**5.34**	**6.84**	**11.41**	**12.68**	**9.98**	**6.47**	**3.1**	**1.52**	**1.15**
	TREND	**1.06**	**2.09**	**5.24**	**6.10**	**6.34**	**11.89**	**10.93**	**8.44**	**7.53**	**3.17**	**1.67**	**1.33**
	OK	**0.84**	**1.89**	**5**	**4.85**	**4.57**	**8.15**	**8.18**	**7.06**	**4.8**	**1.63**	**1.41**	**1.18**
	SPLINE	**0.97**	**1.81**	**7.29**	**6.99**	**7.04**	**12.18**	**12.57**	**9.71**	**6.68**	**2.79**	**1.51**	**1.47**
	REGRESSION	**1.05**	**1.98**	**4.94**	**5.86**	**5.03**	**7.46**	**6.07**	**4.6**	**7.41**	**2.92**	**1.72**	**1.3**
RMSE	IDW	**1.19**	**1.94**	**5.65**	**6.53**	**8.56**	**13.50**	**15.47**	**12.72**	**8.23**	**3.51**	**1.71**	**1.35**
	TREND	**1.28**	**2.22**	**8.13**	**8.88**	**8.52**	**15.01**	**15.80**	**10.52**	**8.23**	**3.88**	**1.88**	**1.79**
	OK	**1.18**	**2.16**	**6.16**	**6.21**	**5.54**	**10.78**	**9.75**	**8.62**	**6.05**	**2.18**	**1.65**	**1.37**
	SPLINE	**2.22**	**8.13**	**8.88**	**8.52**	**15.01**	**15.80**	**10.52**	**8.23**	**3.88**	**1.88**	**1.79**	**2.22**
	REGRESSION	**1.27**	**2.32**	**6.16**	**6.63**	**6.10**	**9.47**	**8.33**	**7.39**	**9.21**	**3.51**	**2.08**	**1.53**

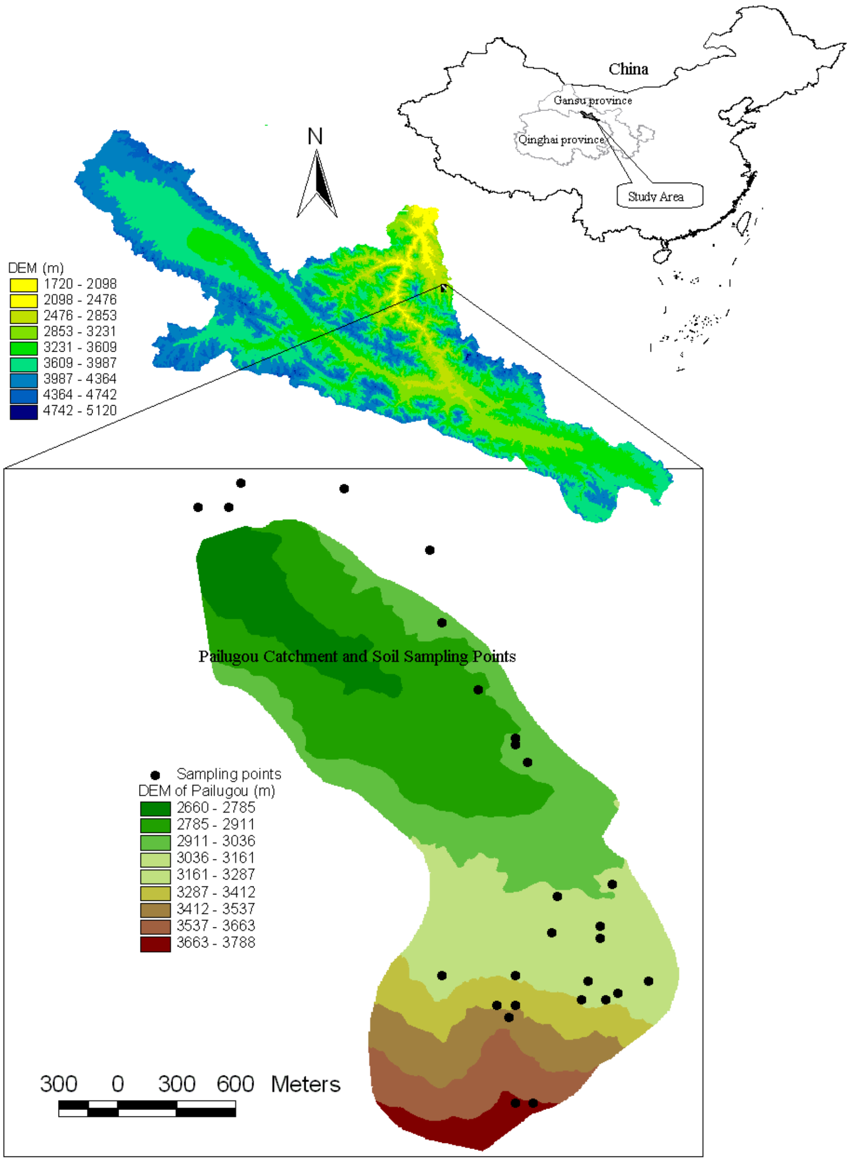

Figure 1. The location of the study area, meteorological stations and rain gauges.

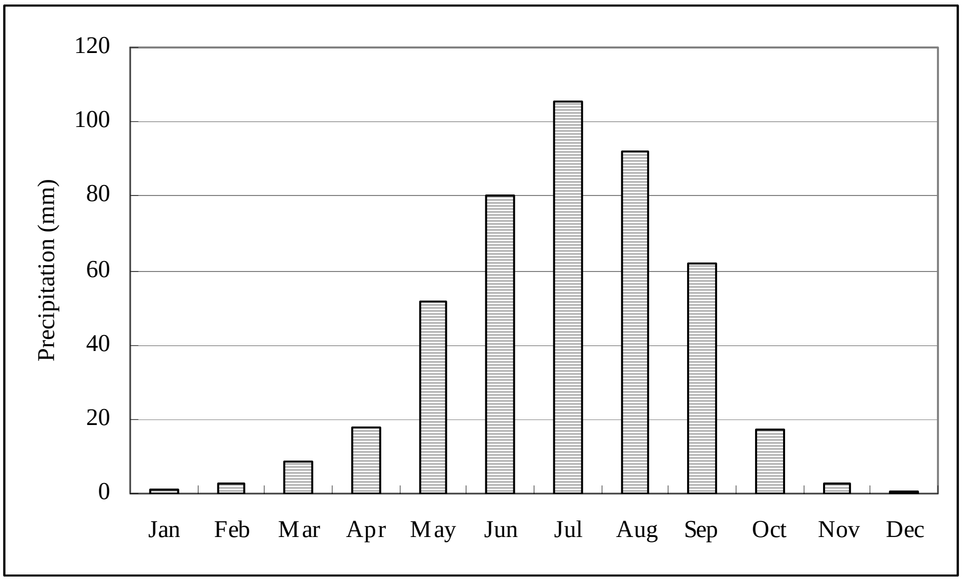

Figure 2. Distribution of monthly mean precipitation in Zhamashike meteorological station (1957-1995).

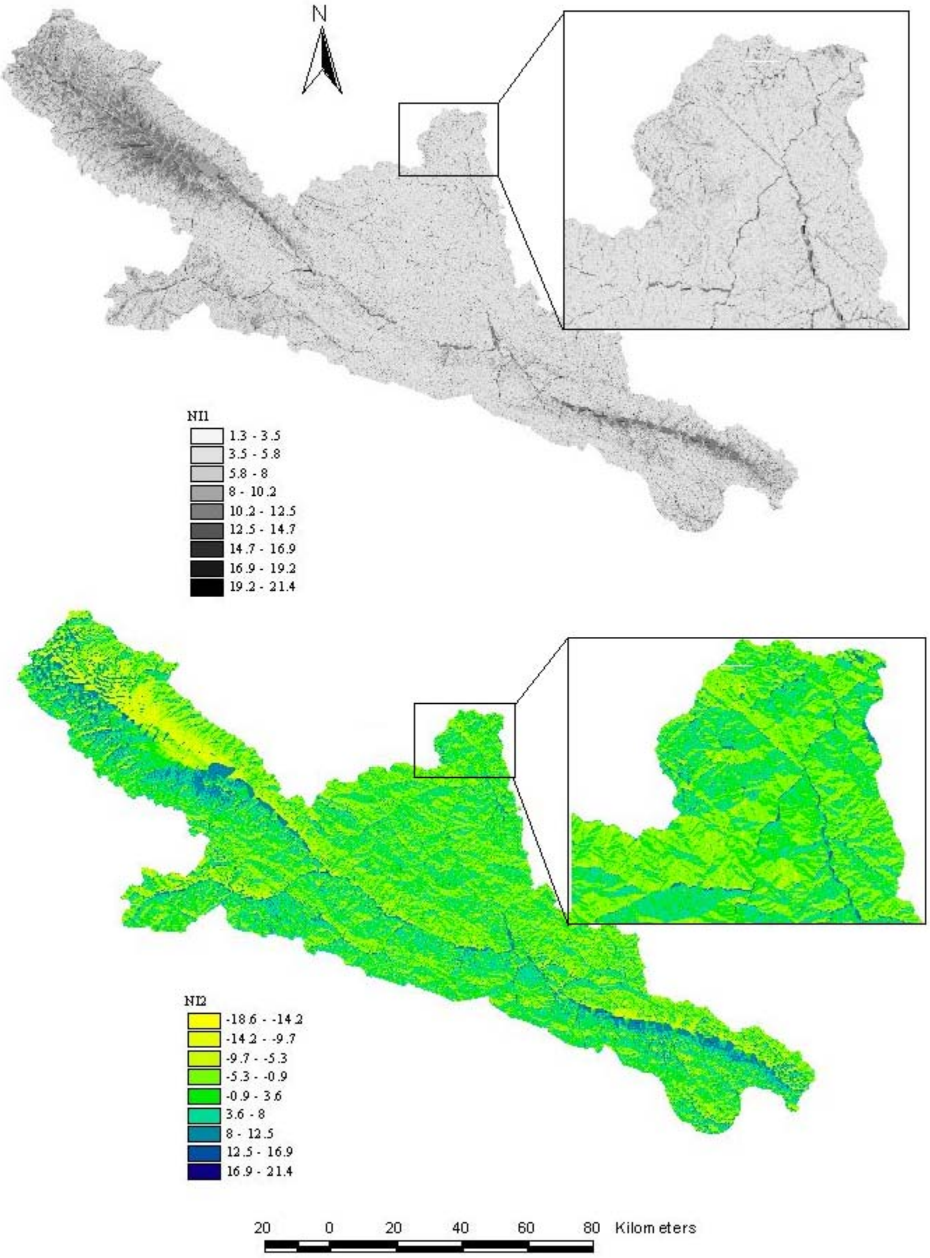

Figure 3. The distribution of wetness indexes (IN_1 and IN_2) in the southern Qilian Mountains.

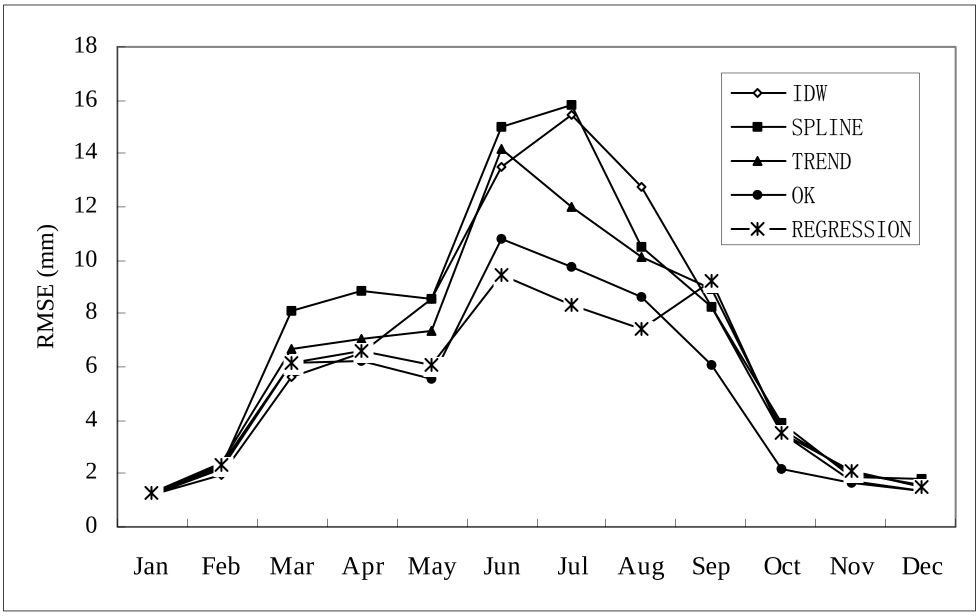

Figure 4. Validation RMSE for monthly mean precipitation averaged across 13 test stations for five methods.

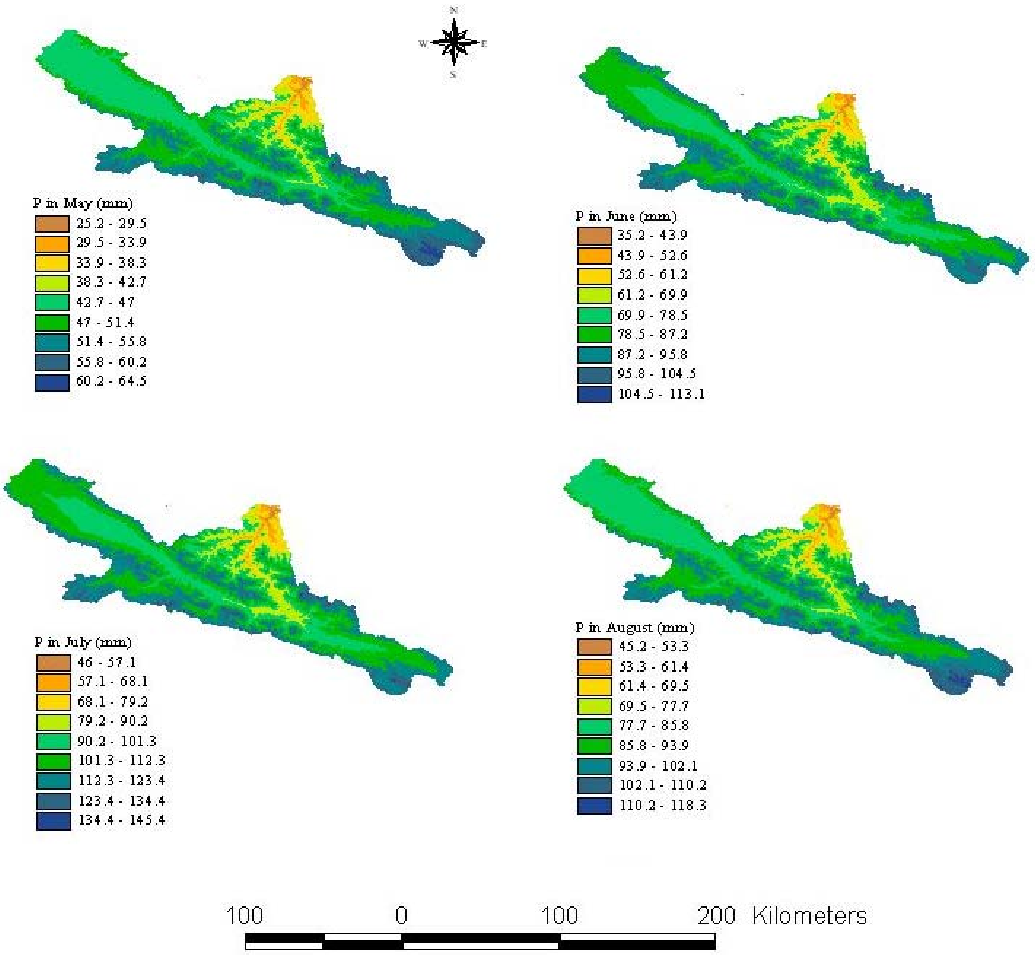

Figure 5 The distribution of monthly mean precipitation in southern Qilian Mountains from May to August.

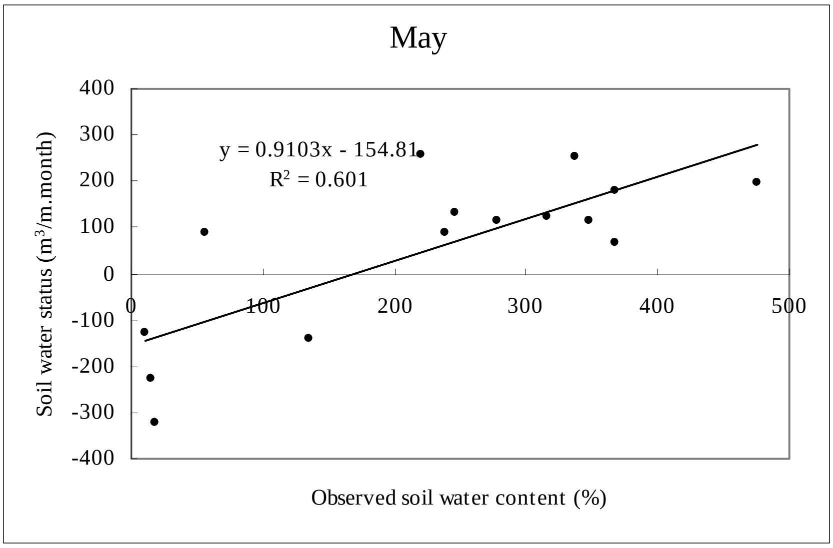
May
y = 0.9103x - 154.81
R^2 = 0.601
Soil water status (m^3/m.month)
Observed soil water content (%)
400
300
200
100
0
-100
-200
-300
-400
0
100
200
300
400
500

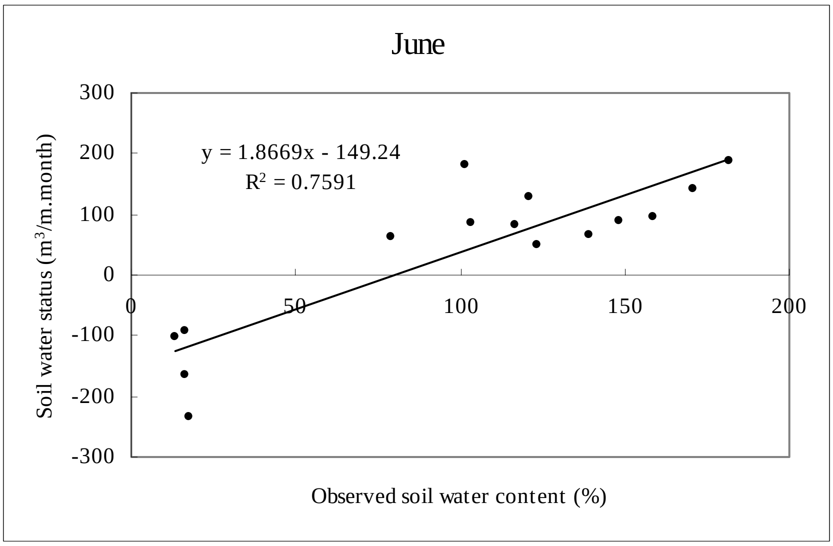
June
y = 1.8669x - 149.24
R^2 = 0.7591
Soil water status (m^3/m.month)
Observed soil water content (%)
300
200
100
0
-100
-200
-300
0
50
100
150
200

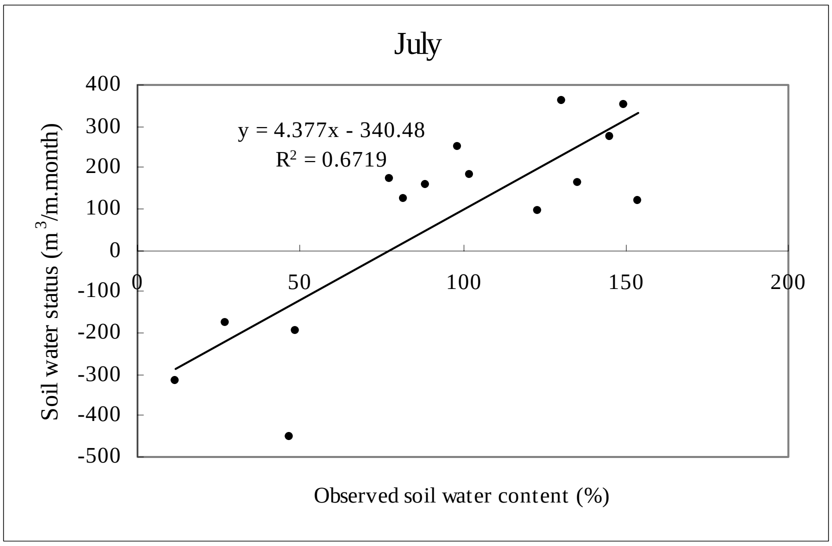
July
y = 4.377x - 340.48
R^2 = 0.6719
Soil water status (m^3/m.month)
Observed soil water content (%)
400
300
200
100
0
-100
-200
-300
-400
-500
0
50
100
150
200

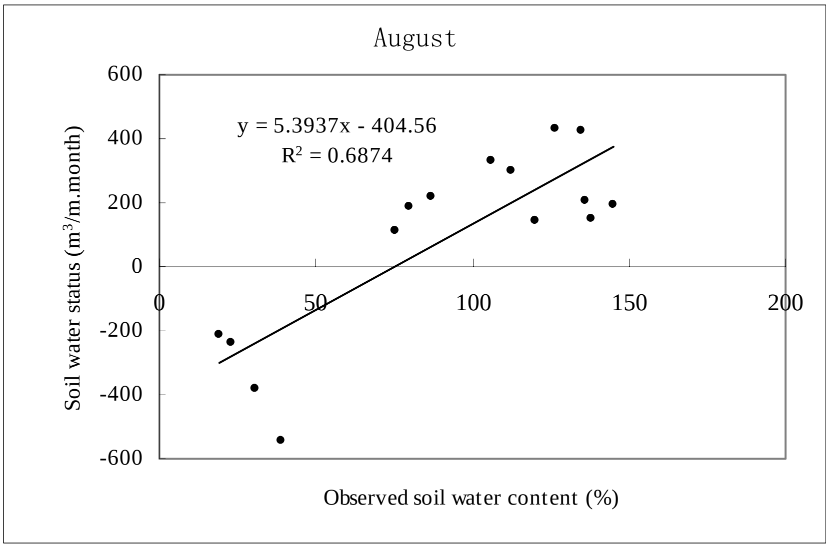

Figure 6. Scatter plots of observed soil moisture content and modeled soil moisture status from May to August

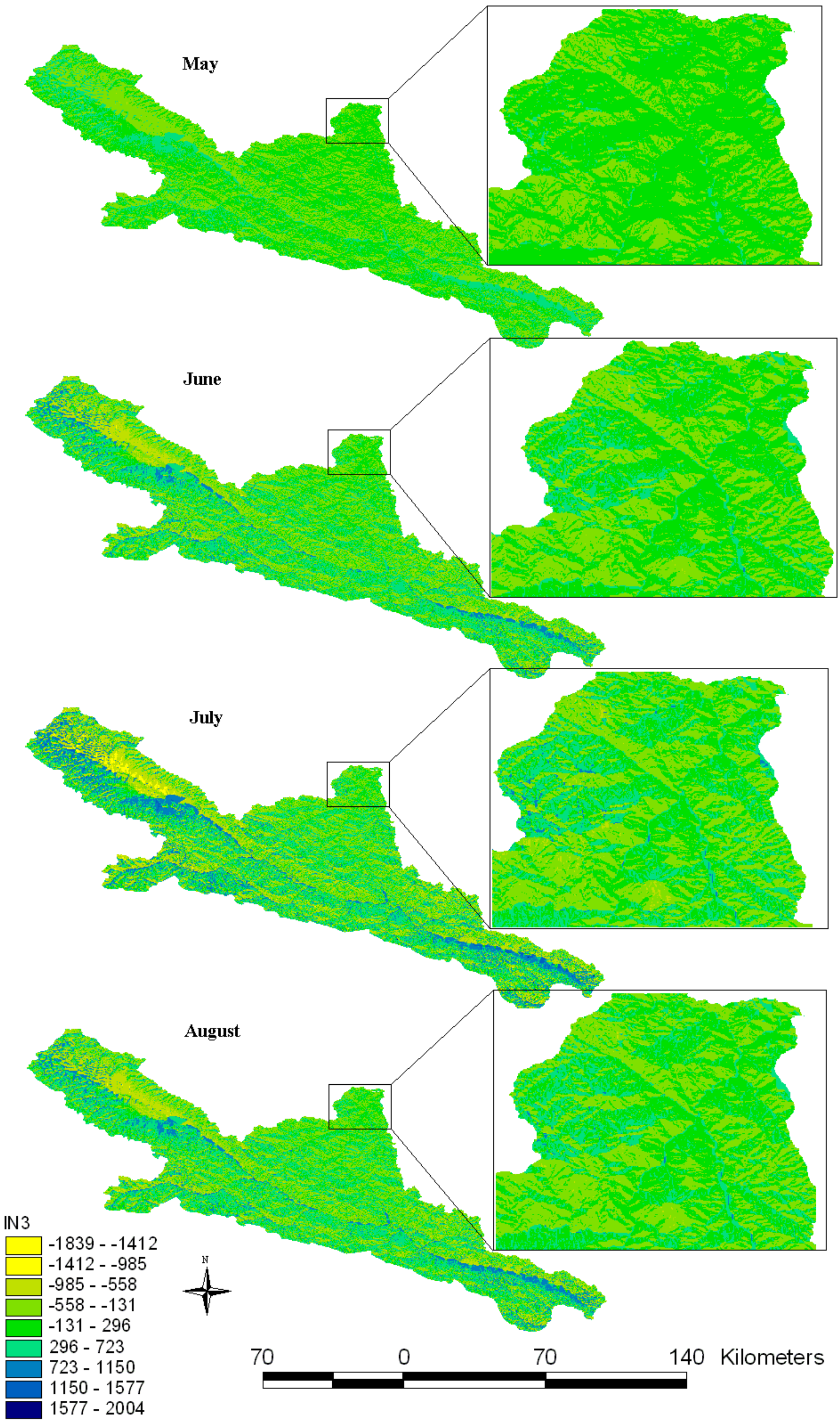

1
2 Figure 7. The distribution of monthly mean soil moisture status in southern Qilian

Mountains from May to August.